

Tunneling Spectroscopy of CdS Schottky-Barrier Junctions*

D. L. LOSEE AND E. L. WOLF

Research Laboratories, Eastman Kodak Company, Rochester, New York 14650

(Received 19 May 1969; revised manuscript received 22 July 1969)

Schottky-barrier tunnel junctions have been fabricated on degenerate CdS by cleavage in high vacuum followed by evaporation of metal contacts. The background conductance of such junctions is found to be in satisfactory agreement with an exact one-electron-model calculation. Polaron effects, observed at biases corresponding to the LO phonon energy, appear to be qualitatively different from published results obtained for junctions on n -type GaAs where electron-phonon coupling is weaker. Zero-bias anomalies of the Appelbaum-Anderson type (conductance peaks) are observed and studied in high magnetic fields. The magnetic field dependence of these anomalies is found to be consistent with the Appelbaum-Anderson model of magnetic scattering as extended by Wolf and Losee. Large negative g shifts of the localized moments are observed.

I. INTRODUCTION

SCHOTTKY-BARRIER junctions formed by intimate contact between a metal and a degenerate semiconductor have recently been examined theoretically^{1,2} and experimentally.³⁻⁵ Such junctions are characterized by a depletion region and band bending near the surface of the semiconductor with no intervening oxide layer between the metal and the semiconductor. For the case of uniform semiconductor doping, the band-edge energies vary quadratically with distance in the depletion region in accordance with the one-dimensional solution of Poisson's equation, the barrier thickness being inversely proportional to the square root of the donor concentration and the barrier height roughly independent of doping.⁶

If the barrier is thin enough (i.e., if the donor concentration is large enough), the dominant charge-transfer mechanism through the junction will be quantum-mechanical tunneling. For the case of parabolic band bending, Conley, Duke, Mahan, and Tiemann¹ (CDMT) have given an exact calculation of the tunneling current in the effective-mass approximation. The recent work of Steinrisser, Davis, and Duke⁵ has shown that the tunneling conductance of junctions formed by cleavage in vacuum of heavily doped Ge is well described by the CDMT model calculation. Thus, it may be said that the Schottky-barrier tunnel-junction conductance provides a well-understood background on which other features in the tunneling current may be superposed.

In the present work, two effects are observed which produce fine structure in the bias dependence of the junction conductance. The first effect, structure at biases corresponding to the CdS LO phonon energy, is related to effects seen in p -type Si⁷ and in p -^{3,8} and n -^{3,9,10} type GaAs and is interpreted as due to structure in the (bulk semiconductor) electron-dispersion relation at energies $\pm\hbar\omega_{LO}$ from the semiconductor Fermi level. In both CdS and n -type GaAs the electron coupling to the LO phonon is screened polar coupling¹¹ but for CdS the coupling constant is a factor of 12 larger than for GaAs. The results obtained here for CdS are qualitatively different from data for n -type GaAs.^{3,9,10} To our knowledge, this is the first report of tunneling measurements for vacuum-cleaved junctions constituted of such a highly polar material.

The second feature is a small (\sim few percent) conductance peak at zero bias of \sim 2-mV width. Such peaks have been observed in Si¹² and GaAs⁸ metal-semiconductor junctions as well as in a number of metal-insulator-metal structures¹³⁻¹⁵ and p - n junctions.^{16,17} Appelbaum¹⁸ and Anderson¹⁹ have attributed these zero-bias anomalies (ZBA) to scattering processes involving conduction electrons interacting with localized magnetic moments in the barrier region. The magnetic field dependence of such ZBA's in Si-Schottky barrier junctions¹² gives support to the Appelbaum-Anderson model of these anomalies. In the present

⁷ E. L. Wolf, Phys. Rev. Letters **20**, 204 (1968).

⁸ D. C. Tsui, Phys. Rev. Letters **21**, 994 (1968).

⁹ C. B. Duke, M. J. Rice, and F. Steinrisser, Phys. Rev. **181**, 733 (1969).

¹⁰ D. C. Tsui, Phys. Rev. Letters **22**, 293 (1969).

¹¹ G. D. Mahan and C. B. Duke, Phys. Rev. **149**, 705 (1966).

¹² E. L. Wolf and D. L. Losee, Solid State Commun. **7**, 665 (1969).

¹³ A. F. G. Wyatt, Phys. Rev. Letters **13**, 401 (1964).

¹⁴ J. M. Rowell and L. Y. L. Shen, Phys. Rev. Letters **17**, 15 (1966).

¹⁵ L. Y. L. Shen and J. M. Rowell, Phys. Rev. **165**, 566 (1968).

¹⁶ R. A. Logan and J. M. Rowell, Phys. Rev. Letters **13**, 404 (1964).

¹⁷ A. G. Chynoweth, R. A. Logan, and D. E. Thomas, Phys. Rev. **125**, 877 (1962).

¹⁸ J. Appelbaum, Phys. Rev. Letters **17**, 91 (1966); Phys. Rev. **154**, 633 (1967).

¹⁹ P. W. Anderson, Phys. Rev. Letters **17**, 95 (1966).

* Work performed in part while authors were guest scientists at Francis Bitter National Magnet Laboratory.

¹ J. W. Conley, C. B. Duke, G. D. Mahan, and J. J. Tiemann, Phys. Rev. **150**, 466 (1966).

² R. Stratton and F. A. Padovani, Phys. Rev. **175**, 1072 (1968); Solid State Electron. **10**, 813 (1967); F. A. Padovani and R. Stratton, Phys. Rev. Letters **16**, 1202 (1966); Appl. Phys. Letters **13**, 167 (1968).

³ J. W. Conley and G. D. Mahan, Phys. Rev. **161**, 681 (1967).

⁴ J. W. Conley and J. J. Tiemann, J. Appl. Phys. **38**, 2880 (1967).

⁵ F. Steinrisser, L. C. Davis, and C. B. Duke, Phys. Rev. **176**, 912 (1968).

⁶ H. K. Henisch, *Rectifying Semiconductor Contacts* (Clarendon Press, Oxford, England, 1957).

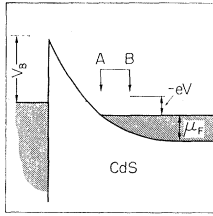


FIG. 1. Schematic diagram of a Schottky barrier on a degenerate n -type semiconductor. V_B is the barrier height; μ_F is the Fermi energy in the semiconductor; V is the applied bias, positive bias corresponds to positive voltage on the metal. The region A-B, where the free-electron density is lower than in the bulk semiconductor, is the region where localized magnetic moments may appear.

work we report high magnetic field studies of ZBA's in CdS junctions which parallel the work done on Si.¹²

II. EXPERIMENTAL

The starting materials used in the present study were single crystals of ultrahigh-purity (UHP) grade CdS purchased from the Eagle-Picher Co., doped with In or Ga. Hall-effect and resistivity measurements²⁰ showed the samples to be degenerate with donor concentrations ranging from 1.7×10^{18} to 6×10^{18} cm^{-3} .

Bars of 0.3×0.3 -cm cross section were cut from the crystals with the c axis transverse to the long axis of the bar. The bars were mounted in a jig and placed in an oil-free, ion-pumped evaporator. Evaporation of Cu, Au or Pb was started. Then, with the sample in the stream of evaporating metal, cleavage was performed with the c axis of the crystal lying parallel to the exposed crystal surface. Since metal is already evaporating, the delay between cleavage and accumulation of metal on the cleavage face is $\lesssim 0.1$ sec, limited by the time required for the front portion of the crystal to fall away. Typical evaporator pressures of $\lesssim 2 \times 10^{-7}$ Torr and evaporation rates of $\gtrsim 10$ $\text{\AA}/\text{sec}$ assured intimate contact between the deposited metal electrode and the CdS crystal, thus eliminating any extraneous chemical contamination. A mask consisting of an array of $150\text{-}\mu\text{m}$ holes, held fixed ~ 2 mm from the point of cleavage, produced an array of evaporated dots on the crystal surface.

After removal of the CdS bar from the evaporator, the end of the bar was again cleaved, producing a small plate of CdS with a number of evaporated junctions. A large-area Ohmic return contact was provided by wetting the back of the CdS plate with an In-Ga amalgam. Such Ohmic return contacts were tested many times and proved to be reliable. They exhibited no detectable non-Ohmic structure in their I - V characteristics. Junction fabrication was performed entirely at temperatures close to room temperature, thus minimizing the chance of impurity redistribution at the surface of the crystal. No significant aging effects have been observed in junctions stored at room temperature for periods up to several weeks.

We believe the vacuum-cleavage procedure is unique in the degree to which the barrier properties and chemical composition are known. Indeed, junctions

²⁰ We are grateful to Dr. R. P. Khosla for kindly performing some of these measurements.

prepared by less well-defined techniques have yielded somewhat different results.²¹

Contact to the evaporated dots was made by lowering a clean spherical gold probe onto a selected dot. Samples were then immersed in liquid helium and their characteristics in terms of dI/dV , d^2I/dV^2 , dV/dI , or d^2V/dI^2 were measured using standard modulation techniques.²² Temperatures as low as 1.2°K were attained and some samples were examined in magnetic fields up to 147 kG. The magnetic field studies were all performed with the field H parallel to the current direction. Modulation levels were low enough so that modulation broadening was usually negligible.

III. JUNCTION CHARACTERIZATION

Figure 1 indicates schematically the electronic band structure of a Schottky-barrier junction with reverse bias applied (metal negative). The capacitance C of such a junction is dependent on applied bias V , barrier height V_B , and the semiconductor donor concentration N_D . A plot of C^{-2} versus V results in a straight-line plot with a voltage-axis intercept nearly equal to the barrier height and slope inversely proportional to the donor concentration.^{3,6,23} Capacitance of a number of junctions was examined at 77°K using an rf impedance bridge, and the results obtained were in good accord with the Schottky-barrier model.

We obtain for barrier heights 0.75 ± 0.1 eV for Au contacts and 0.35 ± 0.1 for Cu. The measurement of the barrier heights is complicated by the large and varying shunt conductance of these junctions. However, the results obtained here are in agreement with the more precise values obtained by Mead and Spitzer,²⁴

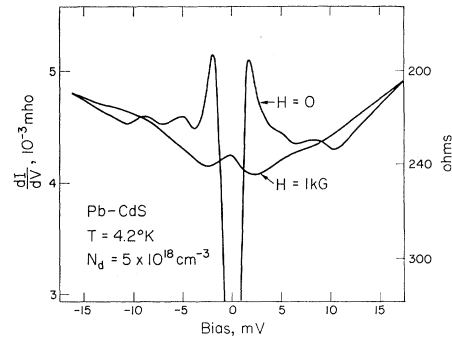


FIG. 2. Expanded view of structure due to the density of states of superconducting Pb at $T=4.2^\circ\text{K}$ on air-cleaved CdS. Structure due to the Pb phonons is apparent. Application of a small magnetic field permits observation of the Appelbaum-Anderson type zero-bias anomaly. The weak structure near ± 5 meV is not understood. It does not appear on vacuum-cleaved junctions with Au or Cu contacts.

²¹ D. L. Losee, *Bull. Am. Phys. Soc.* **13**, 455 (1968); M. Mikkor and W. C. Vassell, *ibid.* **14**, 43 (1969).

²² D. E. Thomas and J. M. Rowell, *Rev. Sci. Instr.* **36**, 1301 (1965); W. R. Patterson and J. Shewchun, *ibid.* **35**, 1704 (1964).

²³ A. M. Goodman, *J. Appl. Phys.* **35**, 573 (1964); **34**, 329 (1963).

²⁴ C. A. Mead and W. G. Spitzer, *Phys. Rev.* **134**, A713 (1964).

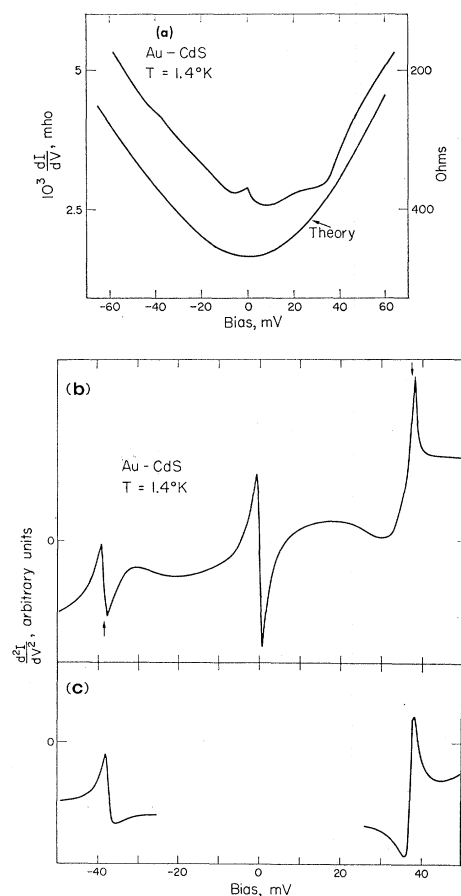


FIG. 3. Tunneling spectra for Au on CdS. (a) $N_D = 5.2 \times 10^{18} \text{ cm}^{-3}$. Semilog plot of dI/dV versus V compared with calculated curve. Parameters used in the calculation are $V_B = 0.80 \text{ eV}$, $m^* = 0.154$, $\epsilon = 8.48$, density-of-states mass $= 0.148$, area $= 5 \times 10^{-4} \text{ cm}^2$. The calculated curve has been adjusted upward by a factor of 6.0 as discussed in the text. Finite distance between sample bar and evaporation mask produced junctions with diameters somewhat greater than the $150\text{-}\mu\text{m}$ mask-hole diameter. (b) $N_D = 5.2 \times 10^{18} \text{ cm}^{-3}$. d^2I/dV^2 versus V for junction of (a) at $T = 1.4^\circ\text{K}$. Arrows indicate $eV = \hbar\omega_{LO}$. The modulation level was 1 mV peak to peak. (c) $N_D = 5.2 \times 10^{18} \text{ cm}^{-3}$. Curve calculated by Davis and Duke (Ref. 32) for screened polar coupling. The parameters used by Davis and Duke for the calculation were $\alpha = 0.5$, $N_D = 5 \times 10^{18} \text{ cm}^{-3}$, $\Gamma_a = 1 \text{ mV}$, $m^* = 0.2$. The parameters are close to those appropriate for the present Au-CdS junction.

0.80 ± 0.05 and $0.35 \pm 0.03 \text{ eV}$ for Au and Cu, respectively, on nondegenerate CdS.

Conclusive evidence that the charge-transfer mechanism is indeed tunneling is given by the observation of proper structure when the contact metal is superconducting Pb. However, for the case of Pb on CdS we have found that cleavage in ultra-high vacuum apparently results in a rather low barrier height. Vacuum-cleaved Pb-CdS junctions fabricated on lightly doped ($1.7 \times 10^{18} \text{ cm}^{-3}$) material resulted in junctions of $\sim 0.5 \Omega$ impedance. dV/dI measurements on these junctions showed proper superconducting structure and proper phonon and zero-bias structure but with a voltage scale significantly distorted by the spreading resistance

of the $\sim 250\text{-}\mu\text{m}$ -diam dot. However, junctions cleaved in air and immediately placed in the evaporator gave barrier heights of $\sim 0.7 \text{ eV}$ and hence more practicable impedance levels. Such air-cleaved Pb-CdS junctions were similar to the vacuum-cleaved junctions in other respects. Figure 2 shows an expanded view of the structure around zero bias for Pb on air-cleaved CdS. The curve obtained with Pb in the superconducting state shows phonon structure in the Pb density of states.²⁵ The ZBA associated with magnetic scattering in the barrier is revealed when a small magnetic field is applied to quench the superconductivity of the Pb.

IV. TUNNELING SPECTRUM

A. Background Conductance

Typical dI/dV data obtained for vacuum-cleaved CdS junctions are shown in Figs. 3(a) and 4(a). Included for comparison is dI/dV calculated on the basis of the CDMT model¹ using the measured donor con-

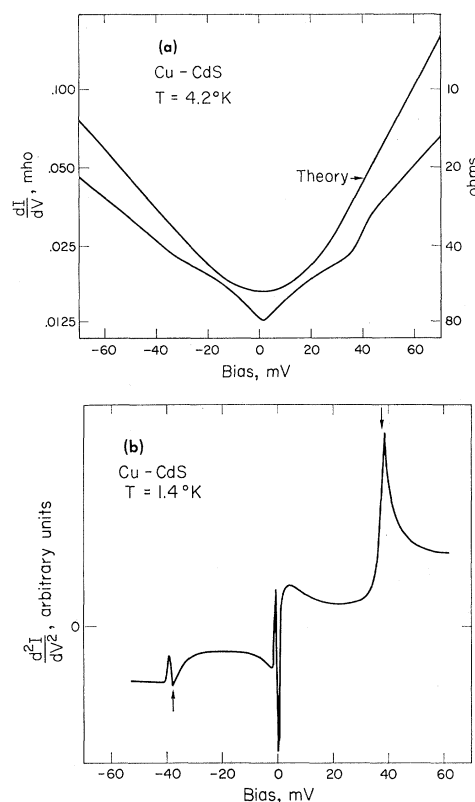


FIG. 4. (a) Tunneling spectrum for Cu on CdS, $N_D = 1.7 \times 10^{18} \text{ cm}^{-3}$. Semilog plot of dI/dV versus V compared with calculated curve. Parameters for the calculated curve are same as for Fig. 3 except $V_B = 0.35 \text{ eV}$ (Ref. 24). No adjustment of the impedance level of the calculated conductance has been made. (b) d^2I/dV^2 versus V for junction of (a) at $T = 1.4^\circ\text{K}$. Arrows indicate $eV = \hbar\omega_{LO}$. Note the increased magnitude of the ZBA at this temperature.

²⁵ For example, see W. L. McMillan and J. M. Rowell, Phys. Rev. Letters 14, 108 (1965).

centrations and literature values for the barrier heights,²⁴ effective mass,²⁶ and dielectric constants.²⁷ In Fig. 3(a), the calculated junction conductance has been multiplied by a constant factor of approximately 6.0 for this comparison. This order of uncertainty in absolute magnitude is not unexpected owing to the great sensitivity of the tunneling conductance level to uncertainty in the barrier height and donor concentration [see Eq. (1) ff, below]. In Fig. 4(a), no such adjustment has been made for the comparison. We consider the agreement to be good. The most important feature, however, is the agreement between theory and experiment for the over-all shape of dI/dV versus bias.

One of the salient features of the CDMT model calculation for the case of the many-valley semiconductors is the occurrence of a minimum in dI/dV at forward bias corresponding to the semiconductor Fermi degeneracy. This feature is conspicuously absent in the present case where the dI/dV minimum occurs at only a few mV positive bias while the Fermi energy μ_F is 74 and 35 meV in the junctions of Figs. 3 and Figs. 4, respectively. The dI/dV minimum calculated by CDMT occurs because electrons at the bottom of the band in the many-valley materials are transmitted through the barrier with almost the same probability as electrons at the Fermi level. CdS, however, has only one conduction-band minimum and thus higher filling of conduction-band levels. There is, therefore, a larger difference in transmission probability between electrons at the top and bottom of the filled conduction-band states. The effect is to move the dI/dV minimum to bias values less than μ_F/e .

In their discussion of Schottky-barrier tunneling Conley and Mahan³ classified junction behavior in terms of two ratios, μ_F/E_0 and eV_B/E_0 , where

$$E_0 = (e^2 N \hbar^2 / 4 m^* \epsilon)^{1/2} \quad (\text{mks units}); \quad (1)$$

and E_0 is the semiconductor band gap. E_0 is an energy parameter appearing in the expression derived for the conductance in the forward bias region, $eV > \mu_F$, where $dI/dV \sim e^{(eV - eV_B)/E_0}$. The CdS junctions studied by us correspond to the case $\mu_F/E_0 \sim 2$ and $V_B/E_0 < \frac{1}{3}$. Conley and Mahan³ found that calculations for junctions having such characteristic ratios exhibit a broad minimum in conductance near zero bias. This observation is in agreement with our calculation and experimental results.

It has been suggested that band-tailing effects might contribute to the appearance of a conductance minimum near zero bias.²⁸ Such effects are more likely to occur in samples with lower donor concentrations and might

²⁶ W. S. Baer and R. N. Dexter, Phys. Rev. **135**, A1388 (1964). We have used the mass values calculated by $m^* = m_p(1 + \alpha/6)^{-1}$, where m_p is the polaron effective mass.

²⁷ D. Berlincourt, H. Jaffe, and L. R. Shiozawa, Phys. Rev. **129**, 1009 (1964). We employ the dielectric constant measured at constant stress at 77°K, ϵ_{11} .

²⁸ G. D. Mahan and J. W. Conley, Appl. Phys. Letters **11**, 29 (1967).

account for the shape of the dI/dV curve of Fig. 4(a) near zero bias. For the junction of Figs. 4 we calculate $\mu_F = 35$ meV $< \hbar\omega_{LO}$ (free-electron approximation) but strong phonon structure at forward bias is still observed. If the band edges were perfectly sharp, however, the phonon structure (as discussed below) should not appear in forward bias.²⁹

B. Phonon Structure

Superposed on the broad bias-dependent background conductance is fine structure near biases corresponding to the LO-phonon energy, $eV = \pm \hbar\omega_{LO} = \pm 37.7$ meV,³⁰ the structure at reverse bias being generally substantially weaker than the forward bias structure. The nature of this structure becomes more evident on examination of d^2I/dV^2 . Figures 3(b) and 4(b) show d^2I/dV^2 measured at $T = 1.4^\circ\text{K}$ for the junctions of Figs. 3(a) and 4(a), respectively. It is seen that the forward bias structure consists of a step in conductance ($\sim 15\%$) with a change in slope, while at reverse bias there occurs structure indicating a conductance peak. We contrast this with the results reported for n -type GaAs. Conley and Mahan³ observed a pair of weak antisymmetric peaks in conductance which were of comparable strength in forward and reverse bias. The details of the structure are somewhat unclear, however, since they show only first derivative data. The recent studies of Duke, Rice, and Steinrisser⁹ and Tsui¹⁰ show d^2I/dV^2 measurements corresponding to a step in conductance at *reverse bias* and a *dip* in conductance at *forward bias*. In both of these reports the phonon structure in the tunneling current is qualitatively different from the data obtained with CdS junctions.

The physical explanation for the appearance of phonon structure is the strong coupling of electrons to the LO phonons ($\alpha = 0.6$ for CdS). This coupling (screened by the electron plasma) produces additional dispersion in the $E(k)$ relation at energies in the vicinity of $\pm \hbar\omega_{LO}$ measured with respect to the semiconductor Fermi level.¹¹ Because the barrier transmission probability, and the phase space available for the tunneling electron, is dependent on $E(k)$, this structure is reflected in the tunneling conductance.^{31,32} Related effects have been observed in p -type Si⁷ and GaAs,⁸ where deformation potential coupling of holes to phonons produces a pair of approximately symmetric peaks in d^2I/dV^2 at the phonon energies. Davis and Duke³¹ have calculated the effect of the hole-LO-phonon coupling for p -type silicon using deformation potential coupling and have found qualitative agreement with the experimental results.⁷ More recently, Davis and Duke³² have performed a similar calculation of d^2I/dV^2

²⁹ L. C. Davis (private communication).

³⁰ B. Tell, T. C. Damen, and S. P. S. Porto, Phys. Rev. **144**, 771 (1966).

³¹ L. C. Davis and C. B. Duke, Solid State Commun. **6**, 193 (1968).

³² L. C. Davis and C. B. Duke (to be published).

for the case of screened polar coupling and their results, displayed in Fig. 3(c), are seen to be in qualitative agreement with the present experimental data.

Inelastic scattering processes may lead to conductance thresholds³³ (which correspond to a pair of antisymmetric peaks in d^2I/dV^2) at biases corresponding to the required excitation energy. The probability for inelastic scattering (coherent and incoherent) should increase with decreasing semiconductor doping.³⁴ However, we observe that in more lightly doped junctions (e.g., Fig. 4), the reverse bias structure is weaker. For this reason, we believe that the inelastic scattering contribution to the d^2I/dV^2 structure is rather weak and we suggest that the structure shown in Figs. 3(b) and 4(b) is primarily due to polaron dispersion.

We mention that in forward bias a rather broad peak in d^2I/dV^2 at about $eV = 2\hbar\omega_{LO}$ is sometimes also observed. There is no corresponding structure in reverse bias so that it is not possible to distinguish which process may be responsible for this peak.

V. ZERO-BIAS ANOMALIES

Prominent in the data shown in Figs. 2–4 is a conductance peak occurring at zero bias. Such peaks have previously been observed in other tunnel junctions^{12–17} and exhibit an approximately logarithmic dependence on temperature and bias. The fact that such peaks are frequently observed in structures with transition metal electrodes led Appelbaum¹⁸ and Anderson¹⁹ to postulate that these anomalous peaks are due to magnetic moments localized in the barrier region near one of the metal electrodes. Recently Wolf and Losee¹² studied such ZBA's in vacuum-cleaved silicon junctions. The systematic dependence of the ZBA parameters on semiconductor donor concentration and the independence of the metal contact species led them to conclude that localized moments are intrinsic in Schottky-barrier junctions and are in fact lightly screened neutral donors at the edge of the depletion region. The arrows in Fig. 1 indicate the region where such localized moments may occur. The magnetic properties of ZBA's in CdS tunnel junctions are discussed below. Our results are consistent with the Appelbaum-Anderson model as extended by Wolf and Losee.¹²

A. ZBA Magnetic Field Dependence

Figure 5 illustrates the typical magnetic field dependence of the ZBA. As the magnetic field strength increases, a dip in conductance develops in the region near zero bias. The conductance change can always be described as a *dip* rather than a splitting since no

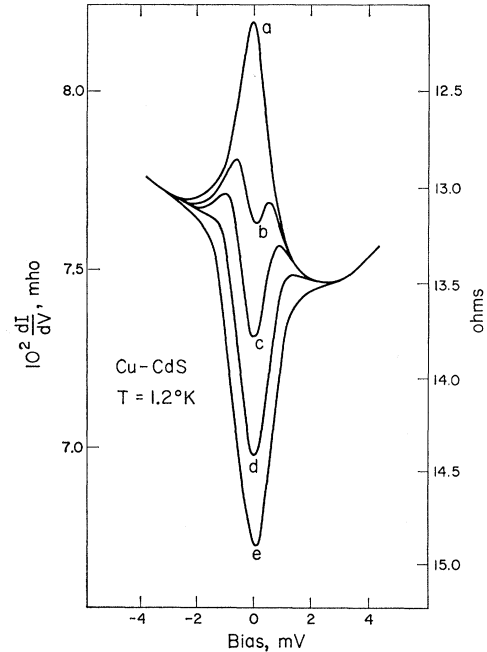


FIG. 5. Zero-bias anomaly for Cu-CdS junction, $N_D = 1.7 \times 10^{18} \text{ cm}^{-3}$, at $T = 1.2^\circ\text{K}$. Magnetic field produces a conductance dip; (a), $H = 0$; (b) 33.2 kG; (c) 66.4 kG; (d) 99.5 kG; (e) 133 kG.

positive regions of ΔG versus bias are observed. Here, we define

$$\Delta G = \left. \frac{dI}{dV} \right|_H - \left. \frac{dI}{dV} \right|_{H=0}. \quad (2)$$

The conductance dip ΔG is examined experimentally in two ways as a function of field strength: (1) dI/dV or dV/dI is measured as a function of H and V and $\Delta G(H, V)$ is determined by direct subtraction of zero-field data; and (2) d^2I/dV^2 or d^2V/dI^2 is measured as a function of V and H , giving $d(\Delta G)/dV$. The second-derivative measurements give additional detail regarding the line shape of the ZBA and may then be integrated to obtain ΔG .

We characterize the ZBA field dependence by the magnitude of the field-induced ΔG and the energy (bias) width at half-depth. Figures 6 and 7 show the field dependence of these parameters for the ZBA of Fig. 5. Two features should be noted: (1) The dip tends toward saturation in magnitude but even at $H = 133 \text{ kG}$ saturation is not complete; (2) the width of the dip asymptotically becomes proportional to field. From the high-field dependence of the width w , we define an apparent g value by the relation

$$w(H) = 2g_{\text{app}}\mu_B H, \quad H \text{ large}. \quad (3)$$

For the junction of Figs. 5–7, we find that $g_{\text{app}} = 0.9 \pm 0.1$, a value typical of all the junctions we have studied.

³³ For example, see R. C. Jaklevic and J. Lambe, Phys. Rev. Letters **17**, 1139 (1966); J. Lambe and R. C. Jaklevic, Phys. Rev. **165**, 821 (1968).

³⁴ C. B. Duke, S. D. Silverstein, and A. J. Bennett, Phys. Rev. Letters **19**, 315 (1967); A. J. Bennett, C. B. Duke, and S. D. Silverstein, Phys. Rev. **176**, 969 (1968).

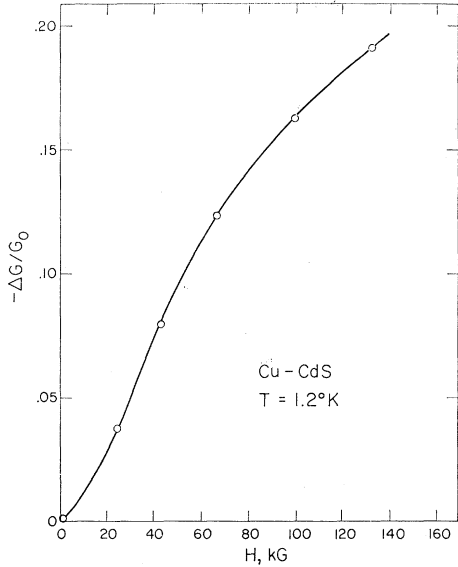


FIG. 6. Relative magnitude of conductance dip versus magnetic field strength for junction of Fig. 5. G_0 corresponds to 13.3Ω .

B. Analysis and Discussion

Appelbaum¹⁸ has treated the problem of magnetic scattering in the barrier within the framework of the tunneling Hamiltonian formalism.³⁵ He finds that first-Born-approximation contributions produce a conductance dip of half-width equal to the Zeeman-level splitting of the localized magnetic moment. This is indicated in Fig. 8(a) [calculated on the basis of Eq. (4) below] and is interpreted physically as a threshold for spin-flip excitation of the local moment.

Extending the calculation to second Born approximation, Appelbaum finds an interference effect which appears in zero-magnetic field as a conductance peak, $G^{(3)}(V)$, and splits into two peaks as a magnetic field is applied. This is illustrated in Fig. 8(b). Analysis of the Appelbaum model¹⁸ yields the following expression for $G^{(2)}$ at finite temperature^{15,36}:

$$G^{(2)} = CTJ^2 \rho_A \rho_B \left\{ S(S+1) - \frac{1}{2} \langle M \rangle \left[h \left(\frac{\Delta + eV}{kT} \right) + h \left(\frac{\Delta - eV}{kT} \right) \right] \right\}, \quad (4a)$$

with

$$h(x) = (-1 + e^{2x} - 2xe^x) / (1 - e^x)^2. \quad (4b)$$

Here, $\Delta = g\mu_B H$ is the Zeeman splitting of the localized-moment energy levels, S is the spin, $\langle M \rangle$ is the average magnetization of the spin system, C is a constant, T_J is the tunneling matrix element for the exchange scattering, and ρ_A and ρ_B are densities of

³⁵ J. Bardeen, Phys. Rev. Letters **6**, 57 (1961); M. H. Cohen, L. M. Falicov, and J. C. Phillips, *ibid.* **8**, 316 (1962).

³⁶ L. Y. L. Shen (unpublished). We are indebted to Dr. Shen for communicating his unpublished calculation.

states on either side of the junction. $\langle M \rangle$ is given by the Brillouin function $B_S(\Delta/kT)$ and is nearly equal to S for $\Delta \gtrsim 4kT$. Thus, for example, with $g=1$ and $T=1.2^\circ\text{K}$, $\langle M \rangle$ should be saturated for $H \gtrsim 70$ kG.

The field dependence of the $G^{(3)}$ peak is given by the following expression¹⁸ in the case of a spin- $\frac{1}{2}$ system:

$$G^{(3)} = -2S(S+1)C\rho_A\rho_B T_J^2 J \times \left\{ \left[\left(\frac{2}{3} - \frac{1}{3} B_{1/2}(\delta) \right) [\tanh(\delta-v) + \tanh(\delta+v)] F(eV) + \left[\frac{2}{3} - \frac{1}{6} B_{1/2}(\delta) \tanh(\delta+v) \right] F(eV + \Delta) + \left[\frac{2}{3} - \frac{1}{6} B_{1/2}(\delta) \tanh(\delta-v) \right] F(eV - \Delta) \right\}, \quad (5)$$

where J is the (antiferromagnetic) exchange energy coupling the localized spin to the electrons in the semiconductor, $B_{1/2}(x) = \tanh \frac{1}{2} x$, $\delta = \Delta/2kT$, $v = eV/2kT$, and $F(eV)$ is a function related to the shape of $G^{(3)}$ in zero field, namely,

$$G^{(3)}(V,0) = -4S(S+1)CTJ^2 J \rho_A \rho_B F(eV) = \text{const} \times F(eV). \quad (6)$$

Appelbaum¹⁸ gives an approximate form for $F(eV)$,

$$F(eV) \approx \rho_A \ln |(eV + kT)/E_1|, \quad (7)$$

where E_1 is an energy parameter, typically several meV. Equation (6), however, provides an experimental determination of the function $F(eV)$. We have found that use of Eqs. (5) and (6) may yield a partially satisfactory separation of $\Delta G^{(2)}$ and $\Delta G^{(3)}$ from the experimentally observed ΔG only for high-field strengths. At lower fields, Eqs. (5) and (6) yield $\Delta G^{(3)}$ values which are too large. By performing such an analysis we find that the effect of $G^{(3)}$ on the field dependence of ΔG is to deepen the conductance dip and to slightly narrow the width at half-depth, i.e., to reduce somewhat the value of g_{app} from the "true" g value which determines the Zeeman energy of the localized magnetic moment.

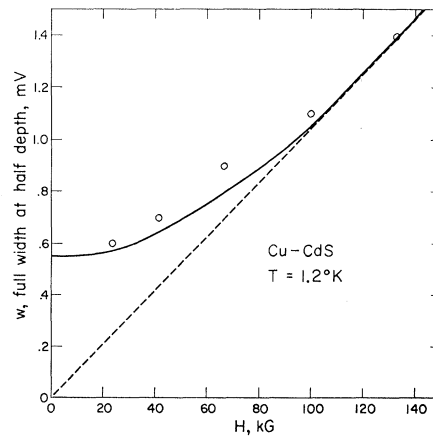


FIG. 7. Full width at half-depth for ΔG of junction shown in Fig. 5. Circles indicate measured values. Solid line shows half-width calculated using Eq. (4) with $g=0.9$, $T=1.2^\circ\text{K}$. Dashed line corresponds to $w = 2g\mu_B H/e$ with $g=0.9$.

Wolf and Losee proposed the following model for the localized magnetic moment in Schottky-barrier junctions.¹² In the semiconductor there exists a region between the degenerate bulk and the depletion region where the free-electron concentration is locally less than the critical Mott concentration for the metal-insulator transition.³⁷ In such a region (about 5 Å wide) localized neutral donor states may exist to produce a localized magnetic moment with g value characteristic of the shallow donor state g_0 . For CdS the shallow donor g value is known from ESR³⁸ and exciton properties³⁹ to be $g_0 \approx 1.78$ and is nearly isotropic. Wolf and Losee¹² have shown that implicit in Appelbaum's treatment of magnetic scattering is a negative g shift resulting from the antiferromagnetic exchange coupling of the neutral donor spins to the conduction electrons in the bulk of the semiconductor. The g shift is given to first order by

$$g - g_0 = \chi_e J / \mu_B^2 = 2J\rho_A(\epsilon_F), \quad (8)$$

where g_0 is the isolated donor g value and ρ_A is the density of the states at the Fermi level in the semiconductor. χ_e is the electronic susceptibility in the semiconductor bulk and μ_B is the Bohr magneton. The second equality results from use of the Pauli expression for χ_e .

The apparent g value observed for the ZBA in CdS junctions is consistent with Eq. (8) although the precise value of $(g - g_0)$ is somewhat uncertain owing to the presence of the relatively large $G^{(3)}$. However, narrowing of ΔG due to $\Delta G^{(3)}$ alone is not sufficient to account for the observed $g_{app} = 0.9 \pm 0.1$. To summarize, for the junctions studied we may roughly estimate the magnitude of the g shift $(g - g_0)$ to be ~ -0.9 . This, in turn, gives a measure of $J\rho_A$. However, we must note that for large $J\rho_A$ the first-order formula, Eq. (8), may be inaccurate. More accurate formulas limited, however, to $T=0$ including higher-order terms, have been given by Wang and Scalapino,⁴⁰ and by Walker.⁴¹

The junctions studied in magnetic fields were of two types; those with $N_D \sim 2 \times 10^{18}$ with Cu contacts and those with $N_D \sim 5-6 \times 10^{18}$ with Au contacts. The junctions with larger N_D exhibited slightly larger $G^{(3)}$ conductance peaks at 1.2°K and approximately equal g_{app} values.

The saturation behavior indicated in Fig. 6 is typical of all CdS tunnel junctions we have studied. A factor leading to the incomplete saturation may be field-

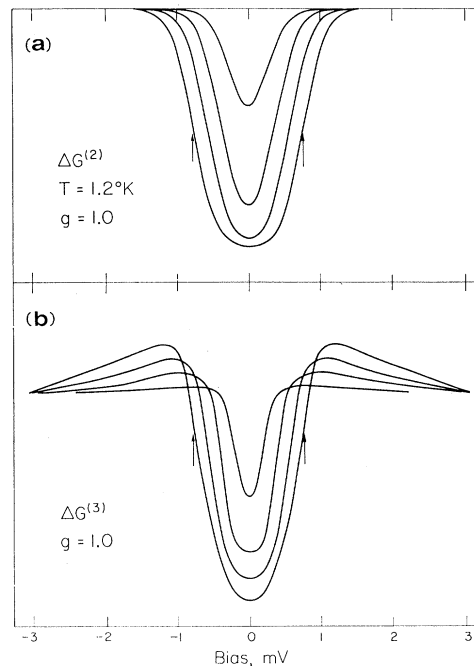


FIG. 8. Magnetic field dependence of $G^{(2)}$ and $G^{(3)}$ contributions to ΔG . (a) $\Delta G^{(2)}$ calculated from Eq. (4) with $T = 1.2^\circ\text{K}$, $H = 33.2, 66.4, 99.5,$ and 133 kG. (b) Predicted $\Delta G^{(3)} = G^{(3)}(H) - G^{(3)}(0)$ with $g = 1.0$, $H = 33.2, 66.4, 99.5,$ and 133 kG, calculated using an experimental zero-field ZBA and Eqs. (5) and (6). Arrows indicate bias where $|eV| = g\mu_B H$ at 133 kG.

induced lifetime broadening of the Zeeman levels of the localized moment. Substantial broadening is expected because of the short "spin-lattice" relaxation time T_1 induced by the exchange scattering process.¹² In analogy with the Knight shift in the NMR of metals,⁴² a "Korringa relation" may be derived^{12,40,41} for the present case where $g\beta H \gg kT$,

$$\hbar/T_1 = \frac{1}{4}\pi(g\mu_B H)(g - g_0)^2(\chi_{0p}/\chi_{p0})^2, \quad (9)$$

which results in $\hbar/T_1 \sim 0.6$ meV when $g\mu_B H = 1$ meV and the last factor in Eq. (9) is taken as unity.

Somewhat more direct experimental evidence for such broadening is given by detailed comparison of the shape of $\Delta G(V)$ with the theoretically predicted shape indicated by Fig. 8(a). Experimentally, we never observe the "flat" region of ΔG at zero bias which is expected at high magnetic fields. Furthermore second-derivative measurements show a broadening of the "line shape" that increases with field as suggested by Eq. (9). These observations are strong evidence that level broadening is an important feature in the description of the localized moment system.

VI. SUMMARY

The technique of vacuum cleavage has been used to fabricate Schottky-barrier tunnel junctions on de-

⁴² C. P. Slichter, *Principles of Magnetic Resonance* (Harper and Row Publishers, Inc., New York, 1963).

³⁷ For an extensive discussion of the Mott transition see Rev. Mod. Phys. **40**, 1 (1968).

³⁸ J. Dielman, in *Magnetic and Electric Resonance and Relaxation, Proceedings of the Colloque AMPÈRE (Atomes et Molécules par les Études Radio-Électriques)*, 1962, edited by J. Smidt (North-Holland Publishing Co., Amsterdam, 1963), p. 409; K. Morigaki, J. Phys. Soc. Japan **19**, 1253 (1964); B. J. Slagsvold and C. F. Schwerdtfeger, Can. J. Phys. **43**, 2092 (1965).

³⁹ J. Hopfield and D. G. Thomas, Phys. Rev. **122**, 35 (1961).

⁴⁰ Y. Wang and D. J. Scalapino, Phys. Rev. **175**, 734 (1968).

⁴¹ M. B. Walker, Phys. Rev. **176**, 432 (1968).

generate CdS crystals. The background conductance of these junctions is well understood on the basis of the work of CDMT.¹ These tunnel junctions exhibit strong structure at biases corresponding to the LO phonon energy which may be understood, at least qualitatively, by consideration of the $E(k)$ relation in the semiconductor as modified by screened polar coupling to the LO phonon. The results are contrasted with existing data on GaAs junctions where the electron-phonon coupling is of the same type but considerably weaker.

Studies of the conductance peaks of the Appelbaum-Anderson type have shown that their magnetic field dependence is consistent with the model of Wolf and Losee¹² for the microscopic origin of the localized

magnetic moments in a Schottky barrier. A large negative g shift is observed for these moments and lifetime broadening effects appear to be important in understanding the detailed structure of the ZBA.

ACKNOWLEDGMENTS

We wish to thank Dr. L. C. Davis for supplying a computer program for the CDMT calculation, and Dr. L. C. Davis and Dr. C. B. Duke for useful discussions and communication of the results of their calculations prior to publication. We wish to thank L. G. Rubin for technical assistance during our visit to the National Magnet Laboratory and Dr. B. C. Cavenett, Dr. R. P. Khosla, and Dr. D. C. Hoesterey for helpful discussions.

Spectroscopic Investigation of Acceptor States in Aluminum Antimonide*

B. T. AHLBURN AND A. K. RAMDAS

Department of Physics, Purdue University, Lafayette, Indiana 47907

(Received 6 June 1969)

Photoexcitation spectra associated with acceptors in p -type aluminum antimonide have been studied. Four sets of sharp photoexcitation lines are observed at liquid-helium temperature; they are absent at liquid-nitrogen or higher temperatures. Equal spacings between pairs of prominent lines in three of these spectra are consistent with an effective-mass-like description for the excited states. The effect of uniaxial stress on several of the acceptor photoexcitation lines has been studied for compressive force \mathbf{F} parallel to $\langle 111 \rangle$ or $\langle 100 \rangle$. The splittings and the polarization patterns may be interpreted if it is assumed that the acceptor centers have T_d site symmetry, and that the bound hole states are not sensitive to a possible departure from a germaniumlike valence band with its maximum at $\mathbf{k}=0$.

I. INTRODUCTION

ACCEPTOR centers can be formed in a III-V compound such as aluminum antimonide in a number of ways. For example, a group-II atom, when substituted for an aluminum atom in the aluminum antimonide lattice can act as an acceptor,¹ as can a group-IV atom substituted for an antimony atom.¹ More complicated acceptor centers, associated with vacancies, interstitial atoms, or clusters of impurities can also be visualized.

Extensive studies of donor and acceptor photoexcitation spectra in germanium^{2,3} and silicon⁴⁻⁶ have demonstrated that significant information about the states

of charge carriers bound to the impurities and about properties of the host crystal can be obtained from such investigations. The application of uniaxial stress, used in conjunction with linearly polarized light, has proven to be of considerable value in interpreting these spectra.⁴⁻⁹ Among the III-V compounds, photoexcitation spectra have been observed for tellurium and selenium donors in aluminum antimonide,¹⁰ manganese acceptors in gallium arsenide,¹¹ and in n -type indium antimonide with the application of high magnetic fields.¹² Preliminary observations of acceptor spectra in gallium antimonide and indium antimonide have also been made.¹³ The authors have presented brief reports¹⁴ on the photoexcitation spectra of acceptors in aluminum

* Work supported by the Advanced Research Projects Agency.
¹ O. Madelung, *Physics of III-V Compounds* (John Wiley & Sons, Inc., New York, 1964), Chap. 5, p. 221.

² J. H. Reuszer and P. Fisher, *Phys. Rev.* **135**, A1125 (1964).

³ R. L. Jones and P. Fisher, *J. Phys. Chem. Solids* **26**, 1125 (1965).

⁴ R. L. Aggarwal and A. K. Ramdas, *Phys. Rev.* **137**, A602 (1965).

⁵ R. L. Aggarwal and A. K. Ramdas, *Phys. Rev.* **140**, A1246 (1965).

⁶ A. Onton, P. Fisher, and A. K. Ramdas, *Phys. Rev.* **163**, 686 (1967).

⁷ R. L. Jones and P. Fisher, *Solid State Commun.* **2**, 369 (1964).

⁸ J. H. Reuszer and P. Fisher, *Phys. Rev.* **140**, A245 (1965).

⁹ D. H. Dickey and J. O. Dimmock, *J. Phys. Chem. Solids* **28**, 529 (1967).

¹⁰ B. T. Ahlburn and A. K. Ramdas, *Phys. Rev.* **167**, 717 (1968).

¹¹ R. A. Chapman and W. G. Hutchinson, *Phys. Rev. Letters* **18**, 443 (1967).

¹² R. Kaplan, *J. Phys. Soc. Japan Suppl.* **21**, 249 (1966).

¹³ P. Fisher (private communication).

¹⁴ B. T. Ahlburn and A. K. Ramdas, *Bull. Am. Phys. Soc.* **14**, 396 (1969); *Phys. Letters* **29A**, 135 (1969).